Virology 498 (2016) 172–180

Contents lists available at ScienceDirect

Virology

journal homepage: www.elsevier.com/locate/yviro

Bioinformatic and mutational analysis of ophiovirus movement proteins, belonging to the 30K superfamily

María Belén Borniego [a,1], David Karlin [b,c,1], Eduardo José Peña [a], Gabriel Robles Luna [a], María Laura García [a,*]

[a] Instituto de Biotecnología y Biología Molecular, CCT—La Plata CONICET, Fac. Cs. Exactas, U.N.L.P., Calles 49 y 115, La Plata, Argentina
[b] Department of Zoology, University of Oxford, Oxford OX1 3PS, UK
[c] The Division of Structural Biology, Henry Wellcome Building, Roosevelt Drive, Oxford OX3 7BN, UK

ARTICLE INFO

Article history:
Received 4 July 2016
Returned to author for revisions
19 August 2016
Accepted 27 August 2016

Keywords:
Movement protein
30K superfamily
Ophiovirus
Negative-strand RNA virus
TMV vector
Citrus psorosis virus
Mirafiori lettuce big-vein virus

ABSTRACT

Ophioviridae is a family of segmented, negative-sense, single-stranded RNA plant viruses. We showed that their cell-to-cell movement protein (MP) is an isolated member of the 30K MP superfamily with a unique structural organization. All 30K MPs share a core domain that contains a nearly-invariant signature aspartate. We examined its role in the MP of *Citrus psorosis virus* (CPsV) and *Mirafiori lettuce big-vein virus* (MiLBVV). Alanine substitution of this aspartate prevented plasmodesmata accumulation of MP^{MiLBVV}, while MP^{CPsV} was not affected. The capacity of ophiovirus MPs to increase the plasmodesmata size exclusion limit and non-cell autonomous protein feature was abolished in both mutants. To investigate the role of the signature aspartate in cell-to-cell movement, we constructed a new movement-deficient Tobacco mosaic virus vector used for trans-complementation assays. We showed that both ophiovirus MP mutants lack the cell-to-cell movement capacity, confirming that this signature aspartate is essential for viral cell-to-cell movement.

1. Introduction

For a successful infection, plants viruses must spread from the first infected cells in a process called cell-to-cell movement until they reach the vasculature and rapidly invade the rest of the plant. This crucial process occurs via plasmodesmata (PD), which are intercellular membranous channels that bridge the cytoplasm of contiguous cells (Heinlein and Epel, 2004). PD conductivity is regulated by the plant in order to control the flow of macromolecules (Crawford and Zambryski, 2001; Lucas et al., 2009; Roberts et al., 2001). In particular, PD only let molecules spread by diffusion if their size is below a cut off the molecular size exclusion limit (SEL), specific to each PD (Ding, 1997). Because the SEL of PDs is always much smaller than the size of any known plant virus or viral genome, plant viruses need an active strategy to cross the PD and move from cell to cell. Most plant viral genomes encode a movement protein (MP) gene(s) that is specifically required for virus spread through PD (Heinlein, 2015; Leisner, 1999; Lucas, 2006).

Many movement proteins display 4 properties that may enable them to mediate viral genome cell-to-cell movement which may be shared by all or most movement proteins. They consist in (1) binding to single-stranded RNA and DNA cooperatively but non-specifically (Karpova et al., 2006; Lough et al., 2000; Shemyakina et al., 2011); (2) localizing to and accumulating at PD (Ding et al., 1992; Lucas, 2006; Niehl and Heinlein, 2011); (3) inducing the increase of the PD size exclusion limit; and (4) facilitating their own or heterologous macromolecules intercellular trafficking (Su et al., 2010; Vogler et al., 2008; Waigmann and Zambryski, 1995; Wolf et al., 1989).

Ophioviridae is a family of negative strand RNA plant viruses whose type specie is *Citrus psorosis virus* (CPsV). Ophioviruses cause major diseases in crops of citrus, lettuce, blueberry and ornamental plants (Moreno et al., 2015; Morikawa et al., 1995; Roggero et al., 2000; Thekke-Veetil et al., 2014; Torok and Vetten, 2010; Vaira et al., 2009; Vaira et al., 1997). Their genome is divided into 3 segments for CPsV and 4 segments for *Mirafiori lettuce big-vein virus* (MiLBVV) (Vaira et al., 2011). RNA 2 encodes the movement protein, named 54K for CPsV and 55K for MiLBVV (Hiraguri et al., 2013; Robles Luna et al., 2013).

MPs are currently grouped in four different structural classes, of which the largest is the 30K superfamily, composed of members structurally related to the 30 kDa MP of *Tobacco mosaic virus* (TMV) (Koonin et al., 1991; Melcher, 2000; Mushegian and Koonin, 1993). While this work was in preparation, Mushegian and Elena (2015)

* Corresponding author.
E-mail address: garcia_m@biol.unlp.edu.ar (M.L. García).
[1] Equal contributor.

http://dx.doi.org/10.1016/j.virol.2016.08.027
0042-6822/

reported that the ophiovirus MP was a member of the 30K superfamily on the basis of sequence analyses. However, in this work we have made a more extensive analysis of the MP, we have delineated the 30K core domain, and we provide biological evidence. MPs of the 30K superfamily have poor overall sequence conservation, but share a conserved core domain with the same predicted secondary structure which consists of 1 α-helix and 7 predicted β-strands (Melcher, 2000; Mushegian and Elena, 2015; Yu et al., 2013). The only sequence feature common to all 30K MPs is a short region between β-strands 1 and 2, which contains several conserved hydrophobic positions, and a nearly-invariant aspartate which constitutes the sequence signature of the superfamily (Melcher, 2000; Mushegian and Koonin, 1993; Yu et al., 2013). This aspartate appears to be required for the movement activity of these MPs (Bertens et al., 2000; Li et al., 2009; Yu et al., 2013; Zhang et al., 2012), but its precise molecular function is unknown.

In a previous study, we demonstrated that the MPs of CPsV and MiLBVV localize to PD, enhance GFP cell-to-cell diffusion, spread to neighboring epidermal cells and can trans-complement cell-to-cell movement of mutants of *Potato virus X* (PVX) and TMV that are defective for movement (Robles Luna et al., 2013). We now asked the following questions: what is the predicted structural organization of the ophiovirus MP? Can it be assigned to a group within the 30K superfamily or it is an isolated member? What is the role of the signature aspartate in ophiovirus MP? We answered these questions by a combination of bioinformatics and biological analyses.

2. Results and discussion

2.1. The ophiovirus MP is an isolated member of the 30K superfamily, and has a unique N-terminal domain

Fig. 1 presents an alignment of the sequences of ophiovirus MPs, with their predicted secondary structure. HHpred (see Methods) on aligned ophiovirus MPs identified a match to PFAM family 3A, which corresponds to the 30K MPs of a wide group of taxa including, among others, *Bromoviridae*, *Virgaviridae* and *Tospoviruses*. This match had a marginal E-value (E=1). We examined it using the software HHalign (Biegert et al., 2006), which is more sensitive, and is used to validate homologs. HHalign returned a statistically significant E-value ($E=7.10^{-4}$) for the comparison between the MPs of ophioviruses and the MPs of the PFAM family 3A, indicating that ophiovirus MPs are homologous to these MPs, and thus are part of the 30K superfamily. While this work was in preparation, Mushegian and Elena (2015) reported similar findings. Examination of the predicted secondary structure of the ophiovirus MP indicates that its core domain (helix αA and strands β1 to β7′ in the nomenclature of Melcher (2000)) is located between amino acids (aa) 90 and 233 in CPsV numbering (Fig. 1, see below). The signature D* residue is boxed in Fig. 1.

In summary, the predicted structural organization of ophiovirus MPs is presented in Fig. 1. They are predicted to be organized in 6 regions (Fig. 1): (1) a disordered N-terminus, variable in sequence and in length (not shown in the alignment); (2) an N-terminal domain conserved in sequence in ophioviruses (strands βX to βZ); (3) the core domain common to all 30K MPs (helix αA and strands β1 to β7′), containing the signature D* residue (boxed in Fig. 1); (4) a long, disordered, central region; (5) a C-terminal domain, conserved in secondary structure but not in sequence; (6) a short, variable disordered C-terminus (not shown in the alignment). The central, disordered region contains two parts: (i) a long segment with the potential to form an α-helix (αB), rich in charged residues, and (ii) a region highly variable in sequence downstream of αB. The first 35 amino acids of the C-terminal domain probably form a highly flexible loop, in view of their sequence variability and low predicted secondary structure content (Fig. 1). Interestingly, we noticed that the C-terminal domain contains a strictly conserved DTG tripeptide (boxed in Fig. 1). It is probably conserved for functional, rather than structural reasons. This conserved tripeptide has not been described in the C-terminus of other 30K MPs, to our knowledge.

We then examined the evolutionary relationship of the ophiovirus MP to other 30K MPs. A Psiblast search on the core domain of ophiovirus MPs found no statistically significant match ($E<10^{-3}$), although it returned a marginal hit (E=3.1) to an MP of the 30K superfamily, the PC4 protein of *Iranian wheat stripe tenuivirus* (accession number AAP82278.1), with 17% sequence identity over 131 aas. By comparison, in a previous study, a Psiblast query on a single 30K MP, that of trichovirus, retrieved most 30K MPs with significant E-values (Mushegian and Elena, 2015). Therefore, the lack of significant matches to ophiovirus MPs in Psiblast clearly indicates that ophiovirus MPs are evolutionarily distant from most other 30K MPs.

At present, the phylogeny of highly distant proteins cannot be reliably inferred, and consequently we could not use the core domain to infer evolutionary relationships between the MP of ophioviruses and that of other 30K MPs. However, one can use derived characters, i.e. characters that are not common to a whole family of proteins, to assess phylogenetic relationships between these proteins. The N-terminal domain of the ophiovirus 30K MP may be such a derived character. Accordingly, we performed homology searches on this N-terminal domain to determine whether we could identify matches to other 30K MPs. We could identify no homologs of this N-terminal domain, even by examining all hits with marginal significance up to an E-value of 10,000 using Psiblast. Therefore, the N-terminal domain is conserved in sequence only in ophioviruses. When combined, the results above clearly indicate that the ophiovirus MP is an isolated member of the 30K superfamily, distantly related to tenuivirus MPs.

2.2. Alanine substitution of the signature aspartate affects differently the PD localization of MPs of CPsV and MiLBVV

To investigate the role of the signature aspartate of the ophiovirus MPs in PD localization, we constructed mutants replacing the aspartate by alanine, generating MP^{CPsV}D141A and MP^{MiLBVV}D174A. We co-expressed the mutants fused to eGFP (MP^{CPsV}D141A:eGFP and MP^{MiLBVV}D174A:eGFP) with the PD marker PDCB1:mCherry in *Nicotiana benthamiana* epidermal cells by agroinfiltration, and visualized their localization by confocal laser scanning microscopy (CLSM). Mutant MP^{CPsV}D141A:eGFP co-localizes with the PD marker, as does the wild-type protein MP^{CPsV}:eGFP (Fig. 2A and B). In contrast, the MP^{MiLBVV}D174A:eGFP mutant did not localize at the PD, but remained localized in the cytoplasm (compare Fig. 2C and D), indicating that the alanine substitution of the aspartate abolishes the localization at PD. Thus, in these two ophioviruses, the signature aspartate plays a different role in the ability of the MP to localize at PD. The expression, size and integrity of the fusion proteins were confirmed by western blot (See Supplementary Fig. 1A).

The effect of substituting the signature aspartate of a 30K MP on localization to the PD has been studied in the genera *Tospovirus*, *Comovirus*, *Emaravirus, Tobamovirus* and *Cytorhabdovirus*. It has been shown that the signature aspartate D154 of the MP (NSm) of the tospovirus *Tomato spotted wilt virus* (TSWV), does not seem to be involved in its subcellular distribution, since when it is replaced by alanine, the cellular distribution of the MP is conserved (Li et al., 2009). In contrast, the substitution D143A in the MP of *Cowpea mosaic virus* reduces its efficiency to target the plasma membrane of the cell (Bertens et al., 2000). Alanine substitution of D127 in the MP of *Raspberry leaf blotch virus* (RLBV) causes loss of

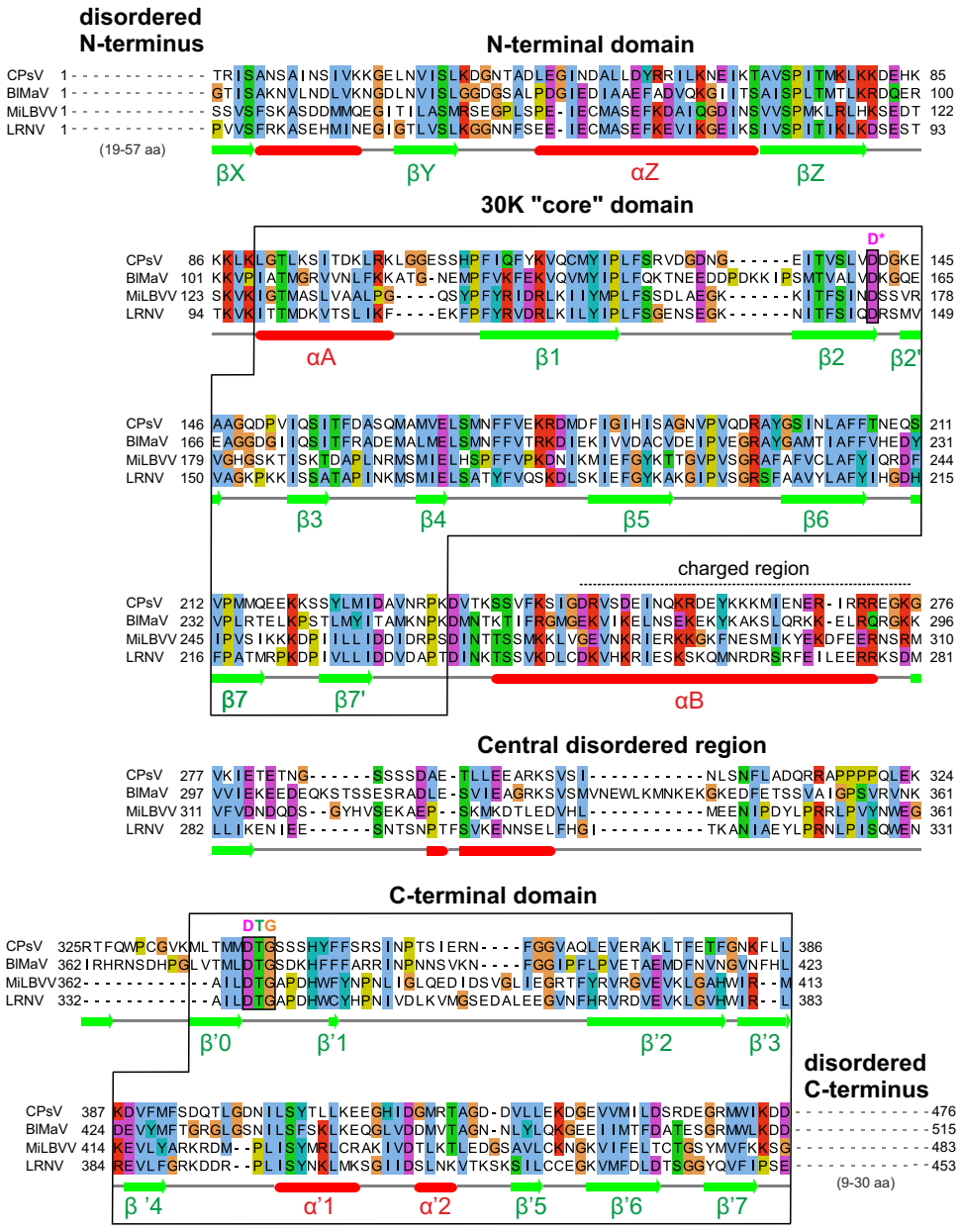

Fig. 1. Sequence alignment and predicted structural organization of ophiovirus MPs. The MPs sequences are those of *Citrus psorosis virus* (CPsV, accession number AAM47152.1), *Mirafiori lettuce big-vein virus* (MiLBVV, accession AGG54707.1), *Blueberry mosaic associated virus* (BlMaV, accession AIF28243.1), and *Lettuce ring necrosis virus* (LRNV, accession YP_053238.1). The boundaries of the central disordered region are approximate. The signature D residue (D*) downstream of β2 and the DTG tripeptide are boxed.

PD localization, although the protein remains associated with membranes (Yu et al., 2013). In the tobamovirus *Turnip vein-clearing virus* (TVCV) the alanine substitution of the signature D103 of its MP (P30) causes the lost of PD localization (Mann et al., 2016). Within the genus *Cytorhabdovirus,* the alanine substitution of the signature D impairs PD targeting of *Lettuce necrotic yellows virus* (LNYV) MP (P3), while the P3 localization of *Alfalfa dwarf virus* (ADV) was mostly unaffected by that substitution (Mann et al., 2016). Thus, this aspartate appears to play no consistent role in subcellular localization, which could explain the contrasting results observed in the two ophiovirus mutants.

2.3. *The signature aspartate of ophiovirus MPs is required to increase the size exclusion limit (SEL) of the plasmodesmata*

It is known that in tobacco sink leaves, but not in source leaves, GFP (27 kDa) and other molecules of up to 50 kDa can diffuse freely through PD (Oparka et al., 1999). We previously showed that MP^{CPsV} and MP^{MiLBVV} are able to increase the PD SEL in source tissues (mature leaves), allowing GFP cell-to-cell diffusion (Robles Luna et al., 2013). We investigated whether the signature aspartate in the MP of both ophioviruses was required for this activity, by using gating assays. We co-infiltrate *Agrobacterium tumefaciens* cultures that allow the expression of GFP and the MPs in *N. benthamiana* source leaves. Isolated cells expressing GFP were achieved by using highly diluted cultures of *Agrobacterium,* while to ensure that all cells of the infiltrated area express either MP^{CPsV}D141A:mRFP, MP^{MiLBVV}D174A: mRFP or mRFP (negative control), the corresponding *Agrobacterium* cultures were used at high concentration. Expression of mRFP fusion proteins was tested by western blot (see Supplementary Fig. 1). Fig. 3A and B(i) show that GFP fluorescent clusters of 2–6 cells were observed in 100% of

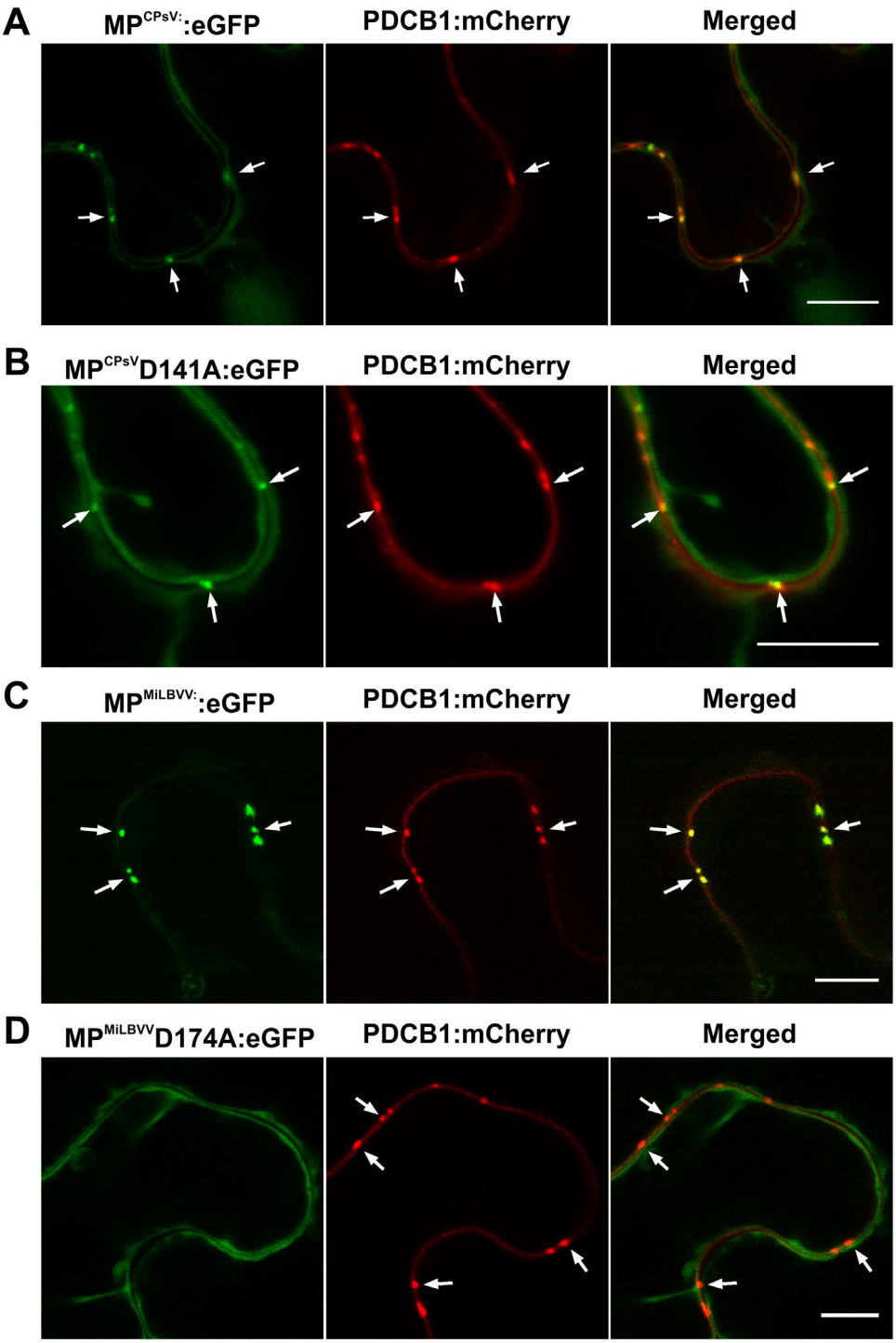

Fig. 2. Subcellular localization of MP^{CPsV}D141A and MP^{MiLBVV}D174A mutants. CLSM at 3 dpai in *N. benthamiana* epidermal cell co-expressing MP^{CPsV}:eGFP (A), MP^{CPsV}D141A:eGFP (B), MP^{MiLBVV}:eGFP (C) or MP^{MiLBVV}D174A:eGFP (D) with PDCB1:mCherry. Scale bar = 10 μm. Arrows indicate PD.

the analysed foci for MP^{CPsV}:mRFP and 67% for MP^{MiLBVV}:mRFP. In contrast, when mutant MPs were co-expressed, fluorescence remained almost exclusively within the transformed cell (14% of foci with 2–3 cells in the case of MP^{CPsV}D141A: mRFP and 11% for MP^{MiLBVV}D174A: mRFP, similar to the negative control). These results indicate that the mutants were not able to facilitate the intercellular passage of GFP. Another feature of ophiovirus MP is their ability to mediate their own transport through PD (Robles Luna et al., 2013), the non-cell autonomous protein (NCAP) feature. Thus, our next goal was to analyse whether the mutants MP^{CPsV}D141A and MP^{MiLBVV}D174A are NCAPs. To address this question, we infiltrated *N. benthamiana* leaves with highly diluted *Agrobacterium* cultures to express either MP^{CPsV}D141A:eGFP or MP^{MiLBVV}D174A:eGFP in isolated epidermal cells. If MP mutants lost the ability to mediate their own transport through PD, GFP fluorescence would remain within the transformed cells. Indeed, GFP fluorescence was observed mainly in isolated cells, with only 16% of foci with 2 or more cells in the case of both MP^{CPsV}D141A:eGFP and MP^{MiLBVV}D174A:eGFP, in contrast to nearly 90% obtained with wild-type MPs (Fig. 3A and B(ii)).

Together, these results indicate that the alanine substitution of the aspartate prevents MPs from modifying the PD SEL, and from

A

		1 cell	2 cells	3 cells	4 cells	5 cells	6 cells	≥7 cells	movement
GFP-gating	GFP + mRFP	84	12	4	0	0	0	0	16
	GFP + MP^{CPsV}:mRFP	0	14	29	0	29	14	14	100
	GFP + MP^{CPsV}D141A:mRFP	86	13	2	0	0	0	0	14
	GFP + MP^{MiLBVV}:mRFP	33	8	17	8	8	8	17	67
	GFP + MP^{MiLBVV}D174A:mRFP	89	11	1	0	0	0	0	11
NCAP	GFP	88	10	2	0	0	0	0	12
	MP^{CPsV}:eGFP	11	9	5	13	4	18	41	89
	MP^{CPsV}D141A:eGFP	84	16	0	0	0	0	0	16
	MP^{MiLBVV}:eGFP	10	4	10	8	0	4	64	90
	MP^{MiLBVV}D174A:eGFP	84	11	3	1	0	0	0	16

B

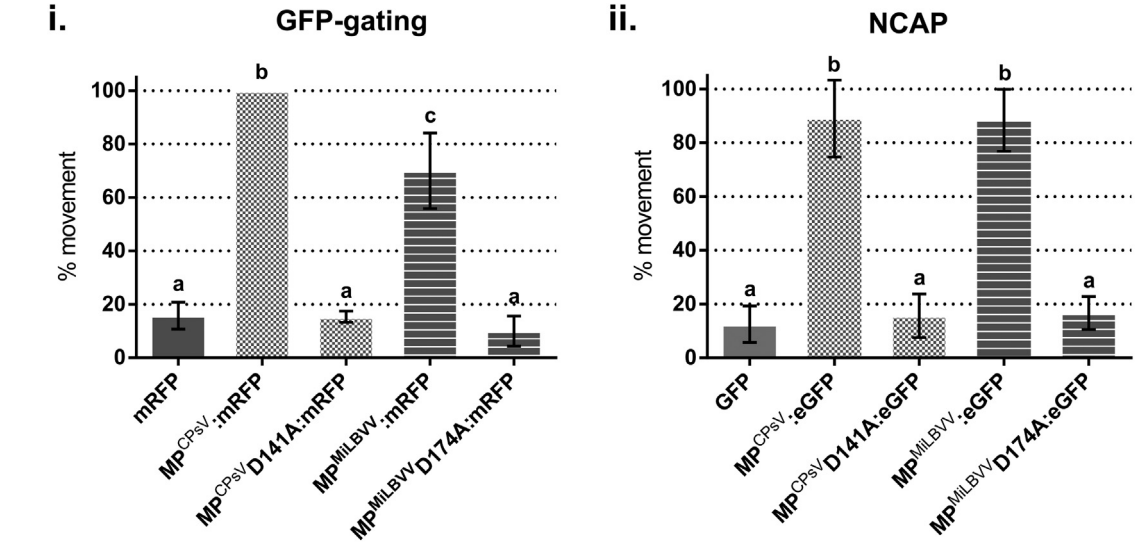

Fig. 3. GFP-gating and NCAP assays of MP^{CPsV}D141A and MP^{MiLBVV}D174A mutants in *N. benthamiana* leaves. (A) Table indicating the percentage of GFP-fluorescent foci at 3 days post agro-infiltration (dpai) with the number of cells in each focus for the conditions described in the left column. Movement = % of foci with GFP signal in ≥2 adjacent cells. (B) Graphs showing the percentage of GFP-fluorescent foci with more than one cell indicating the ability of the mutants to facilitate the intercellular diffusion of cytosolic GFP (i) or to mediate their own transport through PD (NCAP) (ii). Bars represent mean values ± SD from 4 (GFP-gating) or 3 (NCAP) independent experiments. Means with different letters are significantly different (Tukey's HSD, $p < 0.001$).

facilitating their own movement between adjacent cells.

Heinlein (2015) mentioned that the presence of accumulated MP in PD does not necessarily indicate that the PD are gated. Accumulation of MP in PD and gating may even represent independent functions of MP. In this context, the results obtained with the MP^{CPsV}D141A mutant support this idea, since this mutant accumulates at PD but is not able to gate the PD.

2.4. The signature aspartate of ophiovirus MPs is essential for viral movement

We could not perform direct assays of the movement function of MPs in the context of viral infection because an ophiovirus infectious clone system is not available yet. Therefore, we decided to test heterologous viral movement complementation. We created a new TMV-based vector deficient in cell-to-cell movement, which could be used by *Agrobacterium* infiltration rather than in vitro transcription. This vector derived from the pJL-TRBO-G infectious clone (Lindbo, 2007). The vector carries a large N-terminal deletion in its MP, and expresses GFP instead of the coat protein (CP) under the control of the CP subgenomic promoter (TMVΔMPΔCP-GFP) (Fig. 4A(i)). We optimized the conditions for trans-complementation assays using ectopic expression of the MP of TMV (MP^{TMV}) from a binary vector, as positive control (Fig. 4A(ii) and A(iii)). We performed assays by infiltrating *Agrobacterium* culture to express either of each MP fused to mRFP, or free mRFP (used as negative control), together with a diluted *Agrobacterium* culture carrying the TMVΔMPΔCP-GFP vector into *N. benthamiana* leaves. At 5 days post agroinfiltration (dpai), GFP fluorescence was detected only in isolated cells of leaves expressing TMVΔMPΔCP-GFP together with mRFP, showing that this TMV mutant can replicate in the transformed cell but not move to adjacent cells (Fig. 4B (negative controls) and C(i)). In contrast, when TMVΔMPΔCP-GFP was co-expressed with any of the tested MPs, expanding foci of several cells expressing GFP were detected, indicating that the TMV mutant could move efficiently from the original cell into neighboring cells (Fig. 4A(iii), B (positive controls), C(ii) and C(iv)). These results demonstrate that the ectopic expression of MP^{TMV}:mRFP by binary vector was able to complement the cell-to-cell movement of the TMVΔMPΔCP-GFP reporter, indicating that this new vector is functional for trans-complementation assays. As expected, MP^{CPsV}:mRFP and MP^{MiLBVV}:mRFP proteins were also able to restore the movement of the TMV, as we have been previously shown with other two

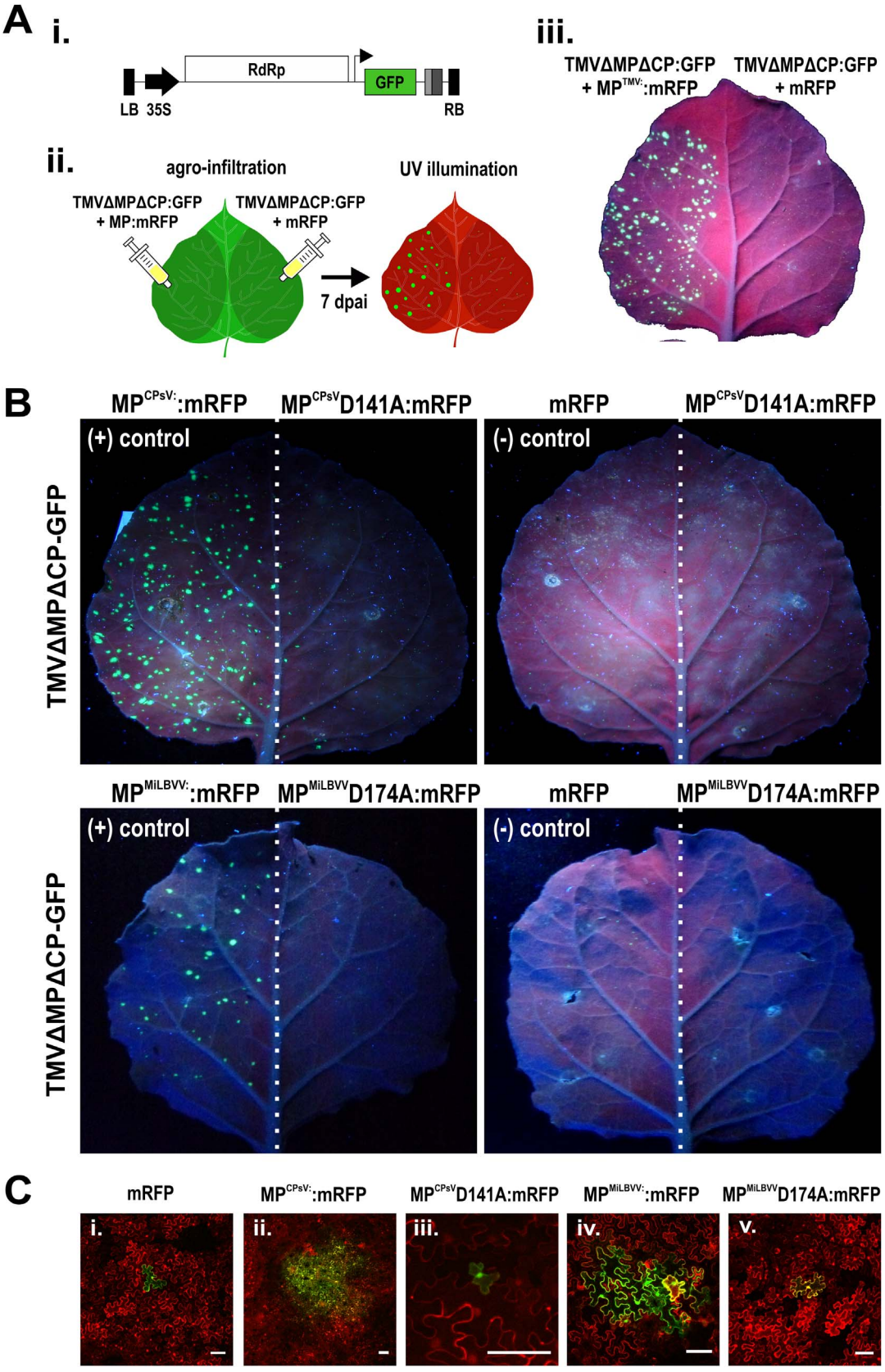

Fig. 4. Movement trans-complementation assay of TMVΔMPΔCP-GFP vector with MP^{CPsV}D141A and MP^{MiLBVV}D174A mutants in *N. benthamiana* leaves. (A) (i) Schematic representation of the T-DNA region of the movement-deficient TMV vector TMVΔMPΔCP-GFP. Block arrow, CaMV duplicated 35S promoter; dark gray box, CaMV polyA signal sequence/terminator; light gray box, Ribozyme; bent arrows, subgenomic promoter. RdRp, TMV 126K/183K ORF; GFP, green fluorescent protein ORF; LB, left border; RB, right border. (ii) Illustration of trans-complementation assay using agro-infiltration (iii) Representative images of UV illuminated *N. benthamiana* leaves co-expressing TMVΔMPΔCP-GFP and MP^{TMV}:mRFP on the left side or mRFP on the right side at 7 dpai. (B) Representative images of UV illuminated *N. benthamiana* leaves co-expressing TMVΔMPΔCP-GFP and the proteins indicated above, taken at 7 dpai. (C) Representative images of the size of TMVΔMPΔCP-GFP infection foci observed on leaves agroinfiltrated for the expression of (i) mRFP, (ii) MP^{CPsV}:mRFP, (iii) MP^{CPsV}D141A:mRFP, (iv) MP^{MiLBVV}:mRFP or (v) MP^{MiLBVV}D174A:mRFP. Fluorescence was monitored with a confocal laser scanning microscope at 5 dpai. Scale bar = 100 μm.

movement-deficient viral vectors (Robles Luna et al., 2013).

To determine the impact of the D mutation in cell-to-cell movement, we conducted the same assay with MP^{CPsV}D141A:mRFP or MP^{MiLBVV}D174A:mRFP mutants. For both mutants, we visualized by GFP fluorescence, foci consisting of single cells (Fig. 4B and C(iii)(v)). Thus, none of these mutants were able to complement the TMVΔMPΔCP-GFP movement mutant, indicating that the signature aspartate is essential for movement complementation. Similar results have been found for the viruses RLBV (*Emaravirus*) (Yu et al., 2013), *Rice stripe virus* (*Tenuivirus*) (Zhang et al., 2012), TSWV (Li et al., 2009), *Tobacco rattle virus* (*Tobravirus*) (Yu et al., 2013), TVCV, ADV and LNYV (Mann et al., 2016), supporting the importance of the signature aspartate for movement function. These results, together with the differences observed in the subcelullar localization, show that PD localization may not be correlated with cell-to-cell movement. Thus, although the signature aspartate seems to be roughly involved in cell-to-cell movement of the 30K MPs, it does not appear to exert the same role on PD localization in all 30K MPs, even between viruses belonging to the same genus as happen with cytorhabdo and ophioviruses.

3. Conclusions

To gain insight into the cell-to-cell movement mechanism of ophioviruses, we realized an exhaustive sequence and structure prediction analysis, together with functional studies on the MPs of this family of negative segmented viruses. We found that the ophiovirus MP is an isolated member of the 30K superfamily, with a unique organization. In ophioviruses, the signature aspartate of the MP is necessary to increase the size exclusion limit of the plasmodesmata, to maintain its NCAP capacity and to support cell-to-cell movement of a movement-deficient TMV virus mutant. In contrast, it is not consistently needed for PD localization in CPsV and MiLBVV. By comparing these results with earlier studies in other virus genera, we can conclude that in the superfamily of 30K MPs, the signature aspartate has a conserved role in the movement activities.

4. Materials and methods

4.1. Protein sequence analyses

We used ANNIE (Ooi et al., 2009) to predict protein structural organization. We used Psi-Coffee (Di Tommaso et al., 2011; Taly et al., 2011) for multiple sequence alignments. The alignment is presented using Jalview (Waterhouse et al., 2009) with the ClustalX colouring scheme (see Fig. 2b and d in Procter et al. (2010)). The secondary structure of individual sequences was predicted using Jpred (Cole et al., 2008), and was verified in the context of multiple alignments using PROMALS (Pei et al., 2007). We predicted disordered regions with MetaDisorder (Kozlowski and Bujnicki, 2012), according to the principles described in (Ferron et al., 2006).

For remote homology detection we used the profile-sequence comparison method Psi-Blast (Altschul et al., 1990; Altschul et al., 1997) and the profile-profile comparison methods HHblits (Remmert et al., 2012) and HHpred (Hildebrand et al., 2009), as described in (Kuchibhatla et al., 2014), against the databases PFAM, version 30 (Finn et al., 2016), with a standard cut-off E-value of 10^{-3}. We used HHalign (Biegert et al., 2006) to validate potential homologs by pairwise comparison, with a cut-off E-value of 10^{-3}.

4.2. Plasmid construction

The wild type MP^{CPsV} and MP^{MiLBVV} fusions constructs and their expression in leaves of *N. benthamiana* were described previously (Robles Luna et al., 2013). MP^{CPsV} and MP^{MiLBVV} mutants were constructed by using overlapping PCR with mutagenic primers and cloned into PCR8/GW/TOPO (ThermoFisher Scientific). The resulting entry plasmids were digested with *XhoI* and recombined with the plant expression vectors pB7RWG2 and pB7FWG2 (Karimi et al., 2002) to obtain C-terminal fusions to mRFP or eGFP, using LR Clonase II Enzyme Mix Kit (ThermoFisher Scientific) following the manufacturer's instructions. Correct cloning was confirmed by DNA sequencing. Verified recombinant plasmids were transferred to *A. tumefaciens* strain GV3101 by electroporation.

TMVΔMPΔCP-GFP was constructed from pJL-TRBO-G (kindly provided by Jonh A. Lindbo) (Lindbo , 2007). A fragment of 489 nt corresponding to the positions 57-545 of the MP was deleted by PCR using *Pfu* DNA polymerase (INBIO Highway) and oligonucleotides: 5′-GGTTACCTAAATAATAGACGGAGGGCCCATGGAAC-3′ and 5′-TCTATTATTTAGGTAACCTTTGTCAGGTCGATAAACTC-3′. The amplified 11 kb PCR product was transformed into *E. coli* strain DH5α. The construct was verified by DNA sequencing and the plasmid transferred to *A. tumefaciens* strain GV3101 by electroporation.

4.3. Plant agroinfiltration

Agroinfiltration experiments were performed in 5 to 6 week old *N. benthamiana* plants maintained in a growth chamber at 23 °C to 25 °C with 16 h light/8 h dark photoperiod. *A. tumefaciens* cultures were harvested by centrifugation, diluted in water to a cell density $OD_{600\ nm}$ value of 0.3 or as indicated, and infiltrated with 1-ml needleless syringe into the abaxial side of the leaf. Leaves were observed at 2–5 days post agroinfiltration (dpai). The expression of the fusion proteins was confirmed by western blot.

4.4. Protein analysis

Total soluble protein extracts of agroinfiltrated plant tissue were prepared by grinding of leaf material frozen in liquid nitrogen and then homogenizing in protein extraction buffer (75 mM Tris–HCl pH 6.8, 10% glycerol, 5% β-mercaptoethanol, 2% SDS and 1.0 mM PMSF) at 4 °C, shaking for 15 min. Extracts were mixed with sample buffer, boiled for 10 min, and clarified by centrifuging for 5 min at 13,000 rpm. Clarified supernatants were separated on 12% [w/v] SDS-PAGE. Proteins were transferred to PVDF membranes (Amersham Hybond-P; GE Healthcare), and blocked with 5% (w/v) nonfat milk powder in Tris-buffered saline containing 0.05% (v/v) Tween-20. eGFP and mRFP fusion proteins were detected with anti-GFP (JL-8) monoclonal antibody (BD Biosciences Clontech, USA) and anti-mRFP [6G6] monoclonal anti body (Chromotek, Germany), respectively. Horseradish Peroxidase conjugated anti-mouse (BioRad, USA) was used as secondary antibody. Protein sizes were estimated using the PageRuler™ pre-stained protein ladder 10–180 kDa (ThermoFisher Scientific).

4.5. Fluorescence microscopy

CLSM was performed using a Leica TCS SP5 II microscope equipped with a HCX PL APO CS 63.0 × 1.40 OIL UV objective, excitation/emission wavelength of 488/524–550 nm for eGFP and of 543/566–634 nm for mRFP, and LAS AF version 2.2.1 4842 software. Images were processed with ImageJ software.

4.6. PD gating assays

PD gating was approached as described previously (Bayne et al., 2005), with minor modifications. Fully expanded leaves of *N. benthamiana* plants were agroinfiltrated with diluted *Agrobacterium* cultures carrying pGDG (for cytosolic GFP expression) (Goodin et al., 2002) at $OD_{600\ nm}=5.0\times10^{-4}$ and the construct that expressed the silencing suppressor p19 (pBin61-P19) (Voinnet et al., 2003) at $OD_{600\ nm}=0.2$ together with *Agrobacterium* cultures carrying the construct that expressed either the negative (mRFP) or positive controls (MP^{CPsV}:mRFP or MP^{MiLBVV}:mRFP) at $OD_{600\ nm}=0.3$ in one half of the leaf allowing GFP expression in isolated epidermal cells, or together with *Agrobacterium* cultures carrying either MP^{CPsV}D141A:mRFP or MP^{MiLBVV}D174A:mRFP ($OD_{600\ nm}=0.3$), on the other side. To evaluate NCAP activity, leaves were co-agroinfiltrated with a diluted *Agrobacterium* culture ($OD_{600\ nm}=5\times10^{-4}$) carrying pGDG, pB7-$MP^{CPsV}$:eGFP, pB7-$MP^{MiLBVV}$:eGFP, pB7-$MP^{CPsV}$D141A:eGFP or pB7-$MP^{MiLBVV}$D174A:eGFP, mixed with an *Agrobacterium* culture carrying pBin61-P19 ($OD_{600\ nm}=0.2$). The number of fluorescence foci and cells in each focus were counted at 3 dpai by fluorescence microscopy. Four (GFP-gating) or three (NCAP) independent experiments were performed. Arcsine transformation was used to correct data for normal distribution. Comparisons among independent experiments for each protein analysed were done using one-way ANOVA (with Tukey's post hoc test, $\alpha=0.05$).

4.7. Movement trans-complementation assay

N. benthamiana leaves were agroinfiltrated with diluted *Agrobacterium* cultures containing TMVΔMPΔCP-GFP ($OD_{600\ nm}=1.0\times10^{-5}$) and pBin61-P19 ($OD_{600\ nm}=0.2$) together with *Agrobacterium* cultures for the expression of either the negative control mRFP ($OD_{600\ nm}=0.3$) or the positive controls (MP^{CPsV}:mRFP or MP^{MiLBVV}:mRFP) ($OD_{600\ nm}=0.3$) in one half of the leaf, or together with *Agrobacterium* cultures carrying either MP^{CPsV}D141A:mRFP or MP^{MiLBVV}D174A:mRFP ($OD_{600\ nm}=0.3$), on the other half. Infection foci were analysed at 4–7 dpai under UV illumination and CLSM. Four independent experiments were done using four leaves for each protein analysed.

Acknowledgments

EJP and MLG are recipients of research career awards from CONICET. MBB and GRL are fellows of CONICET. GRL and MLG belong to the staff of the Facultad de Ciencias Exactas, Universidad Nacional de La Plata, Argentina. This work has been supported by grants from Agencia Nacional de Promoción Científica y Tecnológica (ANPCYT) PICT 2010-1726, PIP 445 Consejo Nacional de Investigaciones Científicas y Técnicas (CONICET) PIP 445, Universidad Nacional de La Plata (UNLP) X692, and by Wellcome Trust grant 090005 to DK. We thank the three anonymous reviewers for their comments, in particular reviewer 3, who was hugely generous in his comments.

Appendix A. Supplementary material

Supplementary data associated with this article can be found in the online version at http://dx.doi.org/10.1016/j.virol.2016.08.027.

References

Altschul, S.F., Gish, W., Miller, W., Myers, E.W., Lipman, D.J., 1990. Basic local alignment search tool. J. Mol. Biol. 215, 403–410.
Altschul, S.F., Madden, T.L., Schaffer, A.A., Zhang, J., Zhang, Z., Miller, W., Lipman, D. J., 1997. Gapped BLAST and PSI-BLAST: a new generation of protein database search programs. Nucleic Acids Res. 25, 3389–3402.
Bayne, E.H., Rakitina, D.V., Morozov, S.Y., Baulcombe, D.C., 2005. Cell-to-cell movement of potato potexvirus X is dependent on suppression of RNA silencing. Plant J. 44, 471–482.
Bertens, P., Wellink, J., Goldbach, R., van Kammen, A., 2000. Mutational analysis of the cowpea mosaic virus movement protein. Virology 267, 199–208.
Biegert, A., Mayer, C., Remmert, M., Soding, J., Lupas, A.N., 2006. The MPI bioinformatics Toolkit for protein sequence analysis. Nucleic Acids Res. 34, W335–W339.
Cole, C., Barber, J.D., Barton, G.J., 2008. The Jpred 3 secondary structure prediction server. Nucleic Acids Res. 36, W197–W201.
Crawford, K.M., Zambryski, P.C., 2001. Non-targeted and targeted protein movement through plasmodesmata in leaves in different developmental and physiological states. Plant Physiol. 125, 1802–1812.
Di Tommaso, P., Moretti, S., Xenarios, I., Orobitg, M., Montanyola, A., Chang, J.M., Taly, J.F., Notredame, C., 2011. T-Coffee: a web server for the multiple sequence alignment of protein and RNA sequences using structural information and homology extension. Nucleic Acids Res. 39, W13–W17.
Ding, B., 1997. Cell-to-cell transport of macromolecules through plasmodesmata: a novel signalling pathway in plants. Trends Cell Biol. 7, 5–9.
Ding, B., Haudenshield, J.S., Hull, R.J., Wolf, S., Beachy, R.N., Lucas, W.J., 1992. Secondary plasmodesmata are specific sites of localization of the tobacco mosaic virus movement protein in transgenic tobacco plants. Plant Cell 4, 915–928.
Ferron, F., Longhi, S., Canard, B., Karlin, D., 2006. A practical overview of protein disorder prediction methods. Proteins 65, 1–14.
Finn, R.D., Coggill, P., Eberhardt, R.Y., Eddy, S.R., Mistry, J., Mitchell, A.L., Potter, S.C., Punta, M., Qureshi, M., Sangrador-Vegas, A., Salazar, G.A., Tate, J., Bateman, A., 2016. The Pfam protein families database: towards a more sustainable future. Nucleic Acids Res. 44, D279–D285.
Goodin, M.M., Dietzgen, R.G., Schichnes, D., Ruzin, S., Jackson, A.O., 2002. pGD vectors: versatile tools for the expression of green and red fluorescent protein fusions in agroinfiltrated plant leaves. Plant J. 31, 375–383.
Heinlein, M., 2015. Plasmodesmata: channels for viruses on the move. Methods Mol. Biol. 1217, 25–52.
Heinlein, M., Epel, B.L., 2004. Macromolecular transport and signaling through plasmodesmata. Int. Rev. Cytol. 235, 93–164.
Hildebrand, A., Remmert, M., Biegert, A., Soding, J., 2009. Fast and accurate automatic structure prediction with HHpred. Proteins 77 (Suppl. 9), S128–S132.
Hiraguri, A., Ueki, S., Kondo, H., Nomiyama, K., Shimizu, T., Ichiki-Uehara, T., Omura, T., Sasaki, N., Nyunoya, H., Sasaya, T., 2013. Identification of a movement protein of Mirafiori lettuce big-vein ophiovirus. J. Gen. Virol. 94, 1145–1150.
Karimi, M., Inze, D., Depicker, A., 2002. GATEWAY vectors for Agrobacterium-mediated plant transformation. Trends Plant Sci. 7, 193–195.
Karpova, O.V., Zayakina, O.V., Arkhipenko, M.V., Sheval, E.V., Kiselyova, O.I., Poljakov, V.Y., Yaminsky, I.V., Rodionova, N.P., Atabekov, J.G., 2006. Potato virus X RNA-mediated assembly of single-tailed ternary 'coat protein-RNA-movement protein' complexes. J. Gen. Virol. 87, 2731–2740.
Koonin, E.V., Mushegian, A.R., Ryabov, E.V., Dolja, V.V., 1991. Diverse groups of plant RNA and DNA viruses share related movement proteins that may possess chaperone-like activity. J. Gen. Virol. 72 (Pt 12), 2895–2903.
Kozlowski, L.P., Bujnicki, J.M., 2012. MetaDisorder: a meta-server for the prediction of intrinsic disorder in proteins. BMC Bioinform. 13, 111.
Kuchibhatla, D.B., Sherman, W.A., Chung, B.Y., Cook, S., Schneider, G., Eisenhaber, B., Karlin, D.G., 2014. Powerful sequence similarity search methods and in-depth manual analyses can identify remote homologs in many apparently "orphan" viral proteins. J. Virol. 88, 10–20.
Leisner, S.M., 1999. Molecular Basis of Virus Transport in Plants. In: Mandahar, C.L. (Ed.), Molecular Biology of Plant Viruses. Springer US, Boston: Kluwer, pp. 161–182.
Li, W., Lewandowski, D.J., Hilf, M.E., Adkins, S., 2009. Identification of domains of the Tomato spotted wilt virus NSm protein involved in tubule formation, movement and symptomatology. Virology 390, 110–121.
Lindbo, J.A., 2007. TRBO: a high-efficiency tobacco mosaic virus RNA-based overexpression vector. Plant Physiol. 145, 1232–1240.
Lough, T.J., Netzler, N.E., Emerson, S.J., Sutherland, P., Carr, F., Beck, D.L., Lucas, W.J., Forster, R.L., 2000. Cell-to-cell movement of potexviruses: evidence for a ribonucleoprotein complex involving the coat protein and first triple gene block protein. Mol. Plant Microbe Interact. 13, 962–974.
Lucas, W.J., 2006. Plant viral movement proteins: agents for cell-to-cell trafficking of viral genomes. Virology 344, 169–184.
Lucas, W.J., Ham, B.K., Kim, J.Y., 2009. Plasmodesmata - bridging the gap between neighboring plant cells. Trends Cell Biol. 19, 495–503.
Mann, K.S., Bejerman, N., Johnson, K.N., Dietzgen, R.G., 2016. Cytorhabdovirus P3 genes encode 30K-like cell-to-cell movement proteins. Virology 489, 20–33.
Melcher, U., 2000. The '30K' superfamily of viral movement proteins. J. Gen. Virol. 81, 257–266.
Moreno, P., Guerri, J., García, M.L., 2015. The psorosis disease of citrus: a pale light at the end of the tunnel. J. Citrus Pathol. 2 (1) ⟨http://escholarship.org/uc/item/0tn7m65m⟩.
Morikawa, T., Nomura, Y., Yamamoto, T., Natsuaki, T., 1995. Partial characterization of virus-like particles associated with tulip mild mottle mosaic. Ann. Phytopathol. Soc. Jpn. 61, 578–581.
Mushegian, A.R., Elena, S.F., 2015. Evolution of plant virus movement proteins from the 30K superfamily and of their homologs integrated in plant genomes.

Virology 476, 304–315.
Mushegian, A.R., Koonin, E.V., 1993. Cell-to-cell movement of plant viruses. Insights from amino acid sequence comparisons of movement proteins and from analogies with cellular transport systems. Arch. Virol. 133, 239–257.
Niehl, A., Heinlein, M., 2011. Cellular pathways for viral transport through plasmodesmata. Protoplasma 248, 75–99.
Ooi, H.S., Kwo, C.Y., Wildpaner, M., Sirota, F.L., Eisenhaber, B., Maurer-Stroh, S., Wong, W.C., Schleiffer, A., Eisenhaber, F., Schneider, G., 2009. ANNIE: integrated de novo protein sequence annotation. Nucleic Acids Res. 37, W435–W440.
Oparka, K.J., Roberts, A.G., Boevink, P., Santa Cruz, S., Roberts, I., Pradel, K.S., Imlau, A., Kotlizky, G., Sauer, N., Epel, B., 1999. Simple, but not branched, plasmodesmata allow the nonspecific trafficking of proteins in developing tobacco leaves. Cell 97, 743–754.
Pei, J., Kim, B.H., Tang, M., Grishin, N.V., 2007. PROMALS web server for accurate multiple protein sequence alignments. Nucleic Acids Res. 35, W649–W652.
Procter, J.B., Thompson, J., Letunic, I., Creevey, C., Jossinet, F., Barton, G.J., 2010. Visualization of multiple alignments, phylogenies and gene family evolution. Nat. Methods 7, S16–S25.
Remmert, M., Biegert, A., Hauser, A., Soding, J., 2012. HHblits: lightning-fast iterative protein sequence searching by HMM-HMM alignment. Nat. Methods 9, 173–175.
Roberts, I.M., Boevink, P., Roberts, A.G., Sauer, N., Reichel, C., Oparka, K.J., 2001. Dynamic changes in the frequency and architecture of plasmodesmata during the sink-source transition in tobacco leaves. Protoplasma 218, 31–44.
Robles Luna, G., Pena, E.J., Borniego, M.B., Heinlein, M., Garcia, M.L., 2013. Ophioviruses CPsV and MiLBVV movement protein is encoded in RNA 2 and interacts with the coat protein. Virology 441, 152–161.
Roggero, P., Ciuffo, M., Vaira, A.M., Accotto, G.P., Masenga, V., Milne, R.G., 2000. An Ophiovirus isolated from lettuce with big-vein symptoms. Arch. Virol. 145, 2629–2642.
Shemyakina, E.A., Solovyev, A.G., Leonova, O.G., Popenko, V.I., Schiemann, J., Morozov, S.Y., 2011. The role of microtubule association in plasmodesmal targeting of potato mop-top virus movement protein TGBp1. Open Virol. J. 5, 1–11.
Su, S., Liu, Z., Chen, C., Zhang, Y., Wang, X., Zhu, L., Miao, L., Wang, X.C., Yuan, M., 2010. Cucumber mosaic virus movement protein severs actin filaments to increase the plasmodesmal size exclusion limit in tobacco. Plant Cell 22, 1373–1387.
Taly, J.F., Magis, C., Bussotti, G., Chang, J.M., Di Tommaso, P., Erb, I., Espinosa-Carrasco, J., Kemena, C., Notredame, C., 2011. Using the T-Coffee package to build multiple sequence alignments of protein, RNA, DNA sequences and 3D structures. Nat. Protoc. 6, 1669–1682.
Thekke-Veetil, T., Ho, T., Keller, K.E., Martin, R.R., Tzanetakis, I.E., 2014. A new ophiovirus is associated with blueberry mosaic disease. Virus Res. 189, 92–96.
Torok, V.A., Vetten, H.J., 2010. Ophiovirus Associated with *Lettuce ring necrosis*. European Society for Virology Meeting. Cernobbio, Italy, p. 282.
Vaira, A.M., García, M.L., Vetten, H.J., Navarro, J.A., Guerri, J., Hammond, J., Verbeek, M., Moreno, P., Natsuaki, T., Gago-Zachert, S., Morikawa, T., Torok, V., Pallás, V., 2011. Ophioviridae. In: King, A.M.Q., Adams, M.J., Carstens, E.B., Lefkowitz, E.J. (Eds.), Virus Taxonomy. IX Report of the International Committee on Taxonomy of Viruses. Elsevier, Oxford (UK), pp. 743–748.
Vaira, A.M., Hansen, M.A., Murphy, C., Reinsel, M.D., Hammond, J., 2009. First report of *Freesia sneak virus* in Freesia sp. in Virginia, USA. Plant Dis. 93, 965.
Vaira, A.M., Milne, R.G., Accotto, G.P., Luisoni, E., Masenga, V., Lisa, V., 1997. Partial characterization of a new virus from ranunculus with a divided RNA genome and circular supercoiled thread-like particles. Arch. Virol. 142, 2131–2146.
Vogler, H., Kwon, M.O., Dang, V., Sambade, A., Fasler, M., Ashby, J., Heinlein, M., 2008. Tobacco mosaic virus movement protein enhances the spread of RNA silencing. PLoS Pathog. 4, e1000038.
Voinnet, O., Rivas, S., Mestre, P., Baulcombe, D., 2003. An enhanced transient expression system in plants based on suppression of gene silencing by the p19 protein of tomato bushy stunt virus. Plant J. 33, 949–956.
Waigmann, E., Zambryski, P., 1995. Tobacco mosaic virus movement protein-mediated protein transport between trichome cells. Plant Cell 7, 2069–2079.
Waterhouse, A.M., Procter, J.B., Martin, D.M., Clamp, M., Barton, G.J., 2009. Jalview Version 2–a multiple sequence alignment editor and analysis workbench. Bioinformatics 25, 1189–1191.
Wolf, S., Deom, C.M., Beachy, R.N., Lucas, W.J., 1989. Movement protein of tobacco mosaic virus modifies plasmodesmatal size exclusion limit. Science 246, 377–379.
Yu, C., Karlin, D.G., Lu, Y., Wright, K., Chen, J., MacFarlane, S., 2013. Experimental and bioinformatic evidence that raspberry leaf blotch emaravirus P4 is a movement protein of the 30K superfamily. J. Gen. Virol. 94, 2117–2128.
Zhang, Y., Zhang, C., Li, W., 2012. The nucleocapsid protein of an enveloped plant virus, Tomato spotted wilt virus, facilitates long-distance movement of Tobacco mosaic virus hybrids. Virus Res. 163, 246–253.